

A computing architecture composed of field-coupled single domain nanomagnets clocked by magnetic field

György Csaba, Wolfgang Porod^{*,†} and Árpád I. Csurgay[‡]

*Center for Nano Science and Technology, Electrical Engineering Department, University of Notre Dame,
275 Fitzpatrick Hall, Notre Dame, IN 46556, U.S.A.*

SUMMARY

Next neighbour field coupling of nanodevices is emerging as an alternative way to integrate nanoelectronic devices (*Nanotechnology* 1993; **4**:49). In this paper, integrated circuits composed of single domain nanomagnets are proposed. New magnetic field-coupled devices with multiple equilibrium states are introduced. The devices are made locally active by exposing them to external magnetic fields. Non-reciprocity is achieved by proper design of the nanomagnet's shape together with its clocking.

We demonstrate that (i) digital signal can propagate along a line of coupled single domain nanomagnets; (ii) and a family of logic circuits (inverter, majority gate, etc.) can be realized. Based on these observations we envision a new nanoelectronic computing architecture as a two-dimensional array of field-coupled nanomagnets. We estimate an integration density of 10^{10} device/cm², few hundred MHz operation speed, straightforward fabrication technology and robust operation in a wide temperature range. Copyright © 2003 John Wiley & Sons, Ltd.

KEY WORDS: nanotechnology; nanoelectronic circuits; micromagnetism

1. INTRODUCTION

Recently the fabrication and characterization technologies of nanomagnets have made remarkable progress [1,2]. The domain structure of magnetic materials has become visible by direct observation using magneto-optical techniques and atomic force microscopes [3]. Concerted efforts are being devoted to develop a hierarchy of descriptive levels of magnetically ordered materials, which can be thought of as an aggregation of elementary magnets, the spins of quantum nature [4–6].

* Correspondence to: Wolfgang Porod, Center for Nano Science and Technology, Electrical Engineering Department, University of Notre Dame, 275 Fitzpatrick Hall, Notre Dame, IN 46556, U.S.A.

† E-mail: porod@nd.edu

‡ On leave from the Budapest University of Technology and Economics and the Pázmány Péter Catholic University, Budapest, Hungary.

Contract/grant sponsor: Office of Naval Research

Contract/grant sponsor: W. M. Keck Foundation

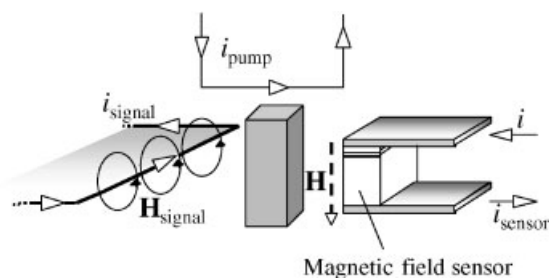


Figure 1. A single nanomagnet as a circuit element. $i_{\text{signal}} = i_z$ and $i_{\text{pump}} = i_y$ determines the fields driving the nanomagnet and its magnetization state is read out by a magnetic field sensor.

In ferromagnetic materials an extraordinarily rich phenomenology arises from the interplay of four different forces, namely the force between magnetic dipoles, the quantum exchange force, the anisotropy force, and the externally applied forces. The force between magnetic dipoles tend to align spins ‘head-to-tail’, thus it exerts a demagnetizing effect. It is a long-range force. It falls off as the third power of the distance between the dipoles. The exchange force, being a ‘per excellence’ quantum effect, tends to align neighbouring spins in parallel. It is short range but very strong force. The anisotropy force tends to align spins along a preferred axis in the material. The external magnetic field is superposed on the above three forces acting on a spin. The internal dynamics of the domain structure arises from the competition between the exchange and the demagnetizing forces.

As long as the material sample is smaller than 1 nm, only an atomic level quantum mechanical model can describe the dynamics. However, if the size of the sample is between 1 nm and 1 μm , the exchange and anisotropy forces can be considered to be phenomenological forces [6]. In this range the internal dynamics of the magnetic material, i.e. the internal structure of the domain walls and their substructures, can be described as the continuum theory of a classical magnetic vector field, called micromagnetic theory or ‘micromagnetism’ [5–7]. In this mesoscopic range only the exchange force represents a quantum effect, all other forces can be considered to be classical. The micromagnetic models describe a mixed quantum-classical dynamics.

In this paper we propose a computing architecture composed of single domain nanomagnets [8–10]. The size of the nanoparticles ranges from 10 to 100 nm, small enough to be single domain but sufficiently large to be stable against thermal fluctuations. The nanomagnets are driven by external magnetic fields, originating from electric currents or neighbouring dots. The single domain magnetization of the dots generates a dipole magnetic field around them, which is measured by a magneto-resistive sensor [11]. Figure 1 shows a nanomagnet with two current inputs generating perpendicular magnetic fields and an output port, which measures the output resistance depending on the dipole field of the nanomagnet. The current generating magnetic field parallel to the easy axis will be the signal input, the current generating magnetic field perpendicular to the easy axis will be the port of the external power source (the pumping or clocking port).

In case of coupled nanomagnets the signal input is replaced by the magnetic fields of the neighbouring nanomagnets.

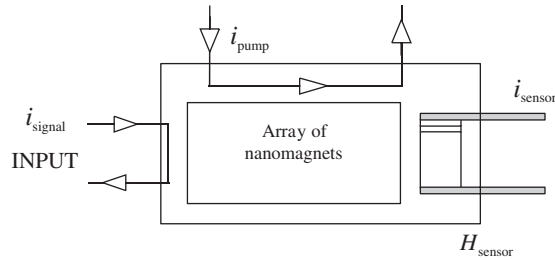


Figure 2. Layout of a nanomagnet circuit array.

This approach gives us the possibility to understand the behaviour of arrays of nanomagnet dots on the basis of circuit concepts.

We envision a nanomagnetic computing architecture [10], which is illustrated in Figure 2. Magnetic field of electric wires provides the input and the pumping field of the array, while in the interior of the array dipole coupling provides the interconnection between elements [14]. Note, that the external magnetic field generating the magnetization inside an individual nanomagnet is the simple superposition of the dipole fields of the neighbours plus the magnetic field of the pumping current. In an array of nanomagnets, the signal field is different for each sample; however, the pumping field is the same for each of them.

The paper is organized in the following way. In Section 2 we rely upon static micromagnetics (outlined in Appendix A), and study the equilibrium characteristics of a single domain nanomagnet as a function of the signal and the pumping input currents.

In Section 3, a dynamic circuit model of a single nanomagnet dot will be introduced. The models are based on the Landau–Lifshitz equations, describing the non-linear quantum-classical dynamics of magnetization in ferromagnetic materials, introduced in Appendix B. We restrict ourselves to the single domain approximation. The device model consists six inductors; their currents represent the magnetization state of the dot. Based on the circuit model, we will illustrate, how the signal field (i_{signal}) can control energy flow between the inductors and the pumping field (i_{pump}).

Section 4 will demonstrate the operation of a set of functional units, serving as nanowires, inverters and majority gates. The proposed devices are clocked by a time-varying magnetic field and function in a quasi-static, adiabatic way if signals change slow enough.

The paper is concluded by the estimation of the achievable speed, dissipation and integration density of the devices. Our detailed field-simulations and measurements by atomic force microscopy on simple circuits composed of permalloy nanomagnets are promising.

2. STATIC I/O CHARACTERISTICS OF A FIELD-DRIVEN SINGLE DOMAIN NANOMAGNET

Let us consider a single domain nanomagnet subject to two current excitations perpendicular to each other (Figure 1), and let us determine the lateral magnetic field H_z generated by the nanomagnet as a function of the two currents, i_{signal} and i_{pump} . The magnetic field H_z can be measured by a sensor, e.g. by a magneto-resistive magnetic field sensor schemati-

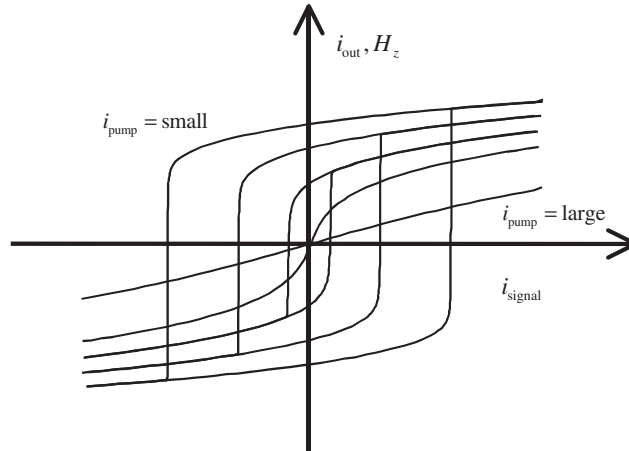


Figure 3. Hysteresis curves of a single domain nanomagnet, characterized by $N_x = N_y = 0.4$ and $N_z = 0.2$.

cally illustrated in Figure 1. This single domain nanomagnet is considered to be the simplest ‘device’.

Characteristics of this device were determined using a single domain micromagnetic model, outlined in Appendix A.

The nanomagnet is a three-port device, its DC characteristics is a two-variable function, $H_z = H_z(i_{\text{signal}}, i_{\text{pump}})$. Figure 3 shows the magnetic field H_z as a function of i_{signal} , for different values of i_{pump} . The longest (easy) axis of the particle lies in the z direction.

For small values of i_{pump} the nanomagnet exhibits almost square-shaped hysteresis loops with two possible equilibrium magnetizations for moderate i_{signal} values. The equilibrium magnetization states are parallel to the easy axis of the particle, and one of them is metastable for $i_{\text{signal}} \neq 0$. As the pumping field increases, the hysteresis loops become narrower and the nanomagnet performs a highly non-linear transition between the metastable and the ground state. For very high pump currents, the hysteresis loop entirely disappears and the nanomagnet responds almost linearly to weak pumping fields.

Applying Biot–Savart law to a particular geometry, we can always express magnetic field values at a given point with an equivalent current which causes the same field and vice versa. For example, the above $H_z = H_z(i_{\text{signal}}, i_{\text{pump}})$ function can be equivalently written as a $H_z = H_z(H_{\text{signal}}, H_{\text{pump}})$ function, where H_{signal} and H_{pump} are the wire-generated magnetic fields affecting the dot. The magnetic field generated by the dot can be represented by an equivalent current, which would affect the sensor in the same way. Therefore, simply rescaling the axes of Figure 3, it could be interpreted as an $i_{\text{out}} = i_{\text{out}}(i_{\text{signal}}, i_{\text{pump}})$ characteristics.

One can define similar characteristics on this function, as on electronic devices. For example, the current (magnetic field) gain of the nanomagnet can be defined as

$$\beta = \frac{di_{\text{out}}}{di_{\text{signal}}} = \frac{dH_{\text{out}}}{dH_{\text{in}}} \quad (1)$$

Note, that the characteristics defined this way are independent of the current-field characteristic of the sensor.

In the next section, we will construct an equivalent circuit of these nanomagnets and interpret their characteristic features.

3. EQUIVALENT CIRCUITS FOR FIELD-COUPLED SINGLE DOMAIN NANOMAGNETS: SIGNAL GAIN AND NON-RECIPROcity

In this section, we will present an equivalent circuit model of a magnetic nanoparticle. The model is based on the single domain Landau–Lifshitz equation, which gives the response (magnetization change) of a nanoparticle subjected to external magnetic fields. The circuit model is based on a physical picture of the energy flow between the nanomagnet and its environment. The concept is illustrated in Figure 4. The magnetization (and the magnetostatic energy) of the dot is subjected to the magnetic field of the wires, and the magnetization change of the dots induces voltages in the wires.

The dynamic behaviour of nanomagnets is modelled by the solution of the time-dependent single domain Landau–Lifshitz equations, discussed in Appendix B. The explicit form of these equations:

$$\begin{aligned}\frac{dM_x(t)}{dt} &= M_s\gamma(H_zM_y - H_yM_z) - M_s\alpha\gamma(H_yM_xM_y - H_xM_y^2 - H_xM_z^2 + H_zM_zM_x) \\ \frac{dM_y(t)}{dt} &= M_s\gamma(H_xM_z - H_zM_x) - M_s\alpha\gamma(H_zM_yM_z - H_yM_z^2 - H_yM_x^2 + H_xM_xM_y) \\ \frac{dM_z(t)}{dt} &= M_s\gamma(H_yM_x - H_xM_y) - M_s\alpha\gamma(H_xM_zM_x - H_zM_x^2 - H_zM_y^2 + H_yM_yM_z)\end{aligned}\quad (2)$$

where M_x , M_y and M_z are the magnetization components of the dot and H_x , H_y , H_z are components of the effective field (both in M_s units). The gyromagnetic ratio is denoted by γ ($\gamma = 2.210 \times 10^5$ m/(As)) and α is a dimensionless damping constant ($\alpha < 1$).

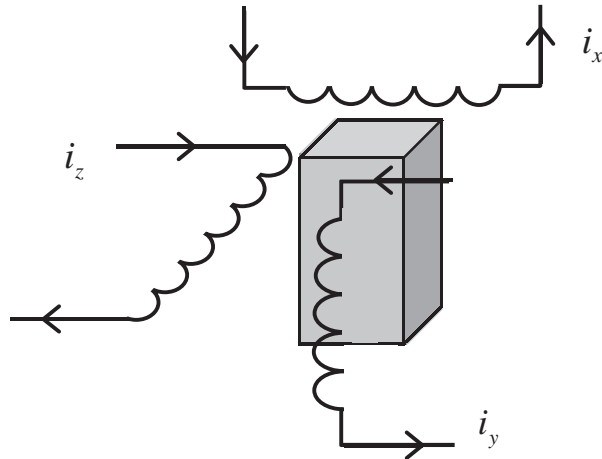


Figure 4. Inductive couplings to the magnetic nanodot.

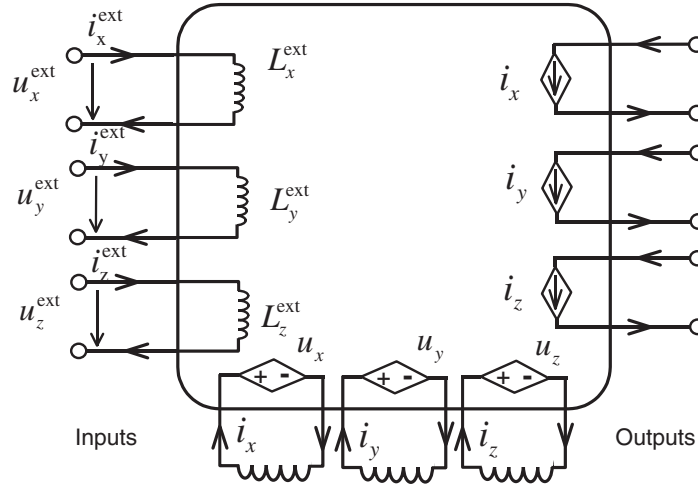


Figure 5. The dynamic circuit model of a nanomagnet. The magnetization components are represented by inductors, which are controlled through a non-linear resistive multiport.

As it is shown in Appendix A, the nanomagnet is characterized by its geometry-dependent demagnetization factors (N_x, N_y, N_z) and volume V , which relate the effective field ($H_x^{\text{ext}}, H_y^{\text{ext}}, H_z^{\text{ext}}$) to the components of the external field (H_x, H_y, H_z) and the magnetization:

$$\begin{aligned} H_x &= H_x^{\text{ext}} - N_x M_x \\ H_y &= H_y^{\text{ext}} - N_y M_y \\ H_z &= H_z^{\text{ext}} - N_z M_z \end{aligned} \quad (3)$$

The equivalent circuit of a single nanomagnet is shown in Figure 5. The magnetization components are considered as currents of the inductors (i_x, i_y, i_z). The values of the inductances are chosen to be equal to the demagnetization factors ($L_x = N_x, L_y = N_y, L_z = N_z$). In this case the self-demagnetization energies corresponding to the different field components are proportional to the energies stored in the inductors:

$$\begin{aligned} E_{L_x} &= \frac{1}{2} L_x i_x^2 = M_s^2 V^2 \frac{1}{2} N_x M_x^2 \\ E_{L_y} &= \frac{1}{2} L_y i_y^2 = M_s^2 V^2 \frac{1}{2} N_y M_y^2 \\ E_{L_z} &= \frac{1}{2} L_z i_z^2 = M_s^2 V^2 \frac{1}{2} N_z M_z^2 \end{aligned} \quad (4)$$

The voltage sources, controlling the inductors can be derived directly from Equation (2):

$$\begin{aligned} u_x &= L_x \gamma M_s ((i_z^{\text{ext}} - L_z i_z) i_y - (i_y^{\text{ext}} - L_y i_y) i_z) - L_x \alpha \gamma M_s ((i_y^{\text{ext}} - L_y i_y) i_x i_y - (i_x^{\text{ext}} - L_x i_x) i_y^2 \\ &\quad - (i_x^{\text{ext}} - L_x i_x) i_z^2 + (i_z^{\text{ext}} - L_z i_z) i_x i_z) \end{aligned}$$

$$\begin{aligned}
u_y &= L_y \gamma M_s ((i_x^{\text{ext}} - L_x i_x) i_z - (i_z^{\text{ext}} - L_z i_z) i_x) - L_y \alpha \gamma M_s ((i_z^{\text{ext}} - L_z i_z) i_y i_z - (i_y^{\text{ext}} - L_y i_y) i_z^2 \\
&\quad - (i_y^{\text{ext}} - L_y i_y) i_x^2 + (i_x^{\text{ext}} - L_x i_x) i_x i_y) \\
u_z &= L_z \gamma M_s ((i_y^{\text{ext}} - L_y i_y) i_x - (i_x^{\text{ext}} - L_x i_x) i_y) - L_z \alpha \gamma M_s ((i_x^{\text{ext}} - L_x i_x) i_z i_x - (i_z^{\text{ext}} - L_z i_z) i_x^2 \\
&\quad - (i_z^{\text{ext}} - L_z i_z) i_y^2 + (i_y^{\text{ext}} - L_y i_y) i_y i_z)
\end{aligned} \tag{5}$$

It is important to note, that the above equations describe a resistive 6-port, and the condition $u_x i_x + u_y i_y + u_z i_z > 0$ holds for any time-independent $i_x^{\text{ext}}, i_y^{\text{ext}}, i_z^{\text{ext}}$ control current.

The inductances at the input of the device ($L_x^{\text{ext}}, L_y^{\text{ext}}, L_z^{\text{ext}}$) represent the Zeeman-energy term, the energy contribution coming from the interaction between external fields and the nanomagnet. These are controlled inductances:

$$\begin{aligned}
L_x^{\text{ext}} &= M_s^2 V^2 \frac{i_x}{i_x^{\text{ext}}} \\
L_y^{\text{ext}} &= M_s^2 V^2 \frac{i_y}{i_y^{\text{ext}}} \\
L_z^{\text{ext}} &= M_s^2 V^2 \frac{i_z}{i_z^{\text{ext}}}
\end{aligned} \tag{6}$$

The energy flow between the inductors is determined by the complex non-linear characteristics of Equation (5). Due to the high non-linearity of the $i_z(i_y^{\text{ext}}, i_z^{\text{ext}})$ characteristics (see Figure 3), the device might exhibit large current gain.

We turn our attention to magnetically coupled nanomagnets, where dots are not accessed individually, but the magnetic field of neighbouring dots serves as input of the inner dots in the structure. In order to keep the model of the individual dot independent of its environment, a coupling circuit between the dots will be introduced, which ‘calculates’ the magnetic field generated by the dots. The coupling field experienced by dot (j) from dot (i) is

$$\begin{bmatrix} i_x^{\text{ext}(j)} \\ i_y^{\text{ext}(j)} \\ i_z^{\text{ext}(j)} \end{bmatrix} = \mathbf{C}^{(ij)} \begin{bmatrix} i_x^{(i)} \\ i_y^{(i)} \\ i_z^{(i)} \end{bmatrix} \tag{7}$$

where the elements of matrix $\mathbf{C}^{(ij)}$ are geometry-dependent constants, and given in Equation (B3). An ideal transformer models this non-energetic 3-port. Note, that due to the reciprocity of the Coulomb coupling, the interaction between two neighbouring dots always requires two transformers with the same coupling matrix. The superposition over multiple field is performed by Kirchhoff’s current law at the input of the dot.

Figure 6 shows quasi-static response of a dot for a small-amplitude oscillating input field (current). The gain defined by Equation (1) is $\beta \approx 2$ in his particular case. This structure is clearly reciprocal: replacing the input and output nodes it exhibits the same transfer characteristics.

Nonreciprocity can be achieved by two coupled, properly designed nanomagnets. Their layout and SPICE simulation is shown in Figure 7. According to the simulations, this circuit shows $\beta > 1$ from its left input to its output and $\beta < 1$ for the reversed input–output position.

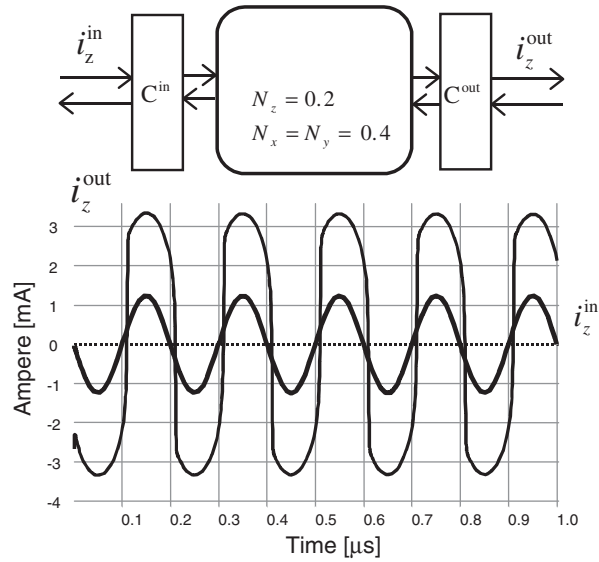


Figure 6. Signal gain of a nanomagnet at constant pump field. The device operates as a magnetic field amplifier. The inset shows the circuit block-diagram.

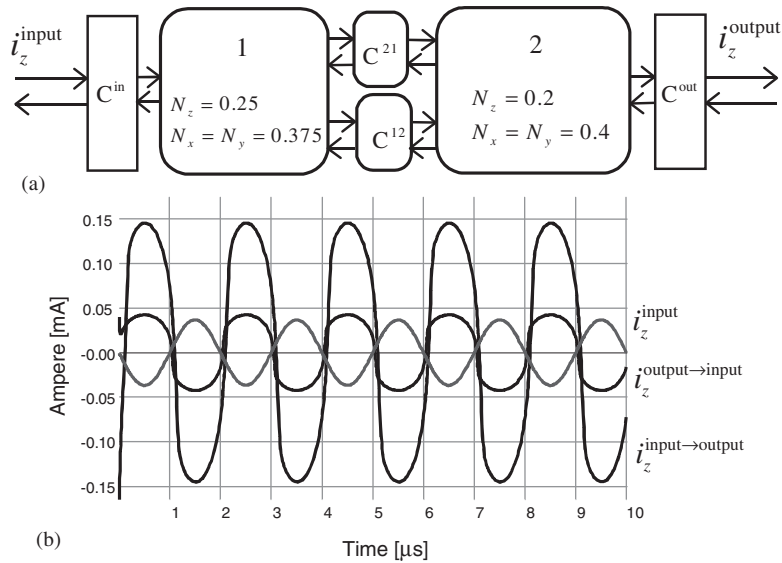


Figure 7. Circuit schematics (a) and quasi-static simulation (b) of a non-reciprocal double-dot is shown. The device shows asymmetric current gain.

4. EXAMPLES OF NANOMAGNET LOGIC CIRCUITS: NANO-WIRE AND MAJORITY GATE

In this section, we will show that a complete set of logic devices that can be built from field coupled nanomagnets. The dots are elongated-shape, and the zero field, steady-state magnetization directions are parallel to the easy (longest) axis. We assign a logic value of '1' to the magnetization pointing up and logical '0' if points down.

The magnetic nanowire is a one-dimensional structure built up from identical dots. With a high-enough magnetic field, the magnetizations of all dots are parallel to the pump field, representing an undetermined logic value (the origin on the characteristic curves in Figure 3). Applying a weak input signal it slightly changes the magnetization of the first dot in the structure. At a certain value of the pump field, the high signal gain propagates the signal through the structure and the wire goes to its magnetically ordered ground state according to the input current. This structure transmits binary information in an entirely magnetic way and wires of odd number of dot serves as an inverter. If the demagnetization factors and the distances of the dots are exactly the same, then this pumping scheme reliably moves the system to its lowest energy state. Figure 8 shows the normalized magnetization (i_{signal}) and pumping currents (i_{pump}) of a particular simulation.

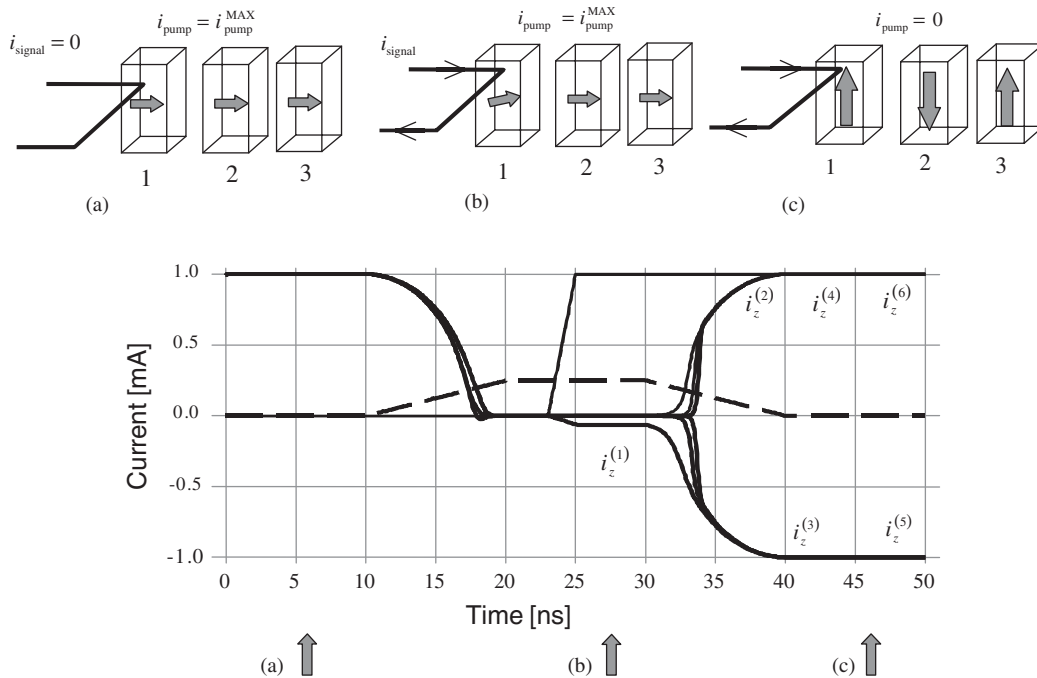


Figure 8. Operation of the magnetic nanowire, as it results from a time-dependent, quasi-static simulation. The insets (a), (b), (c) illustrates the different pumping phases and the corresponding points on the simulation.

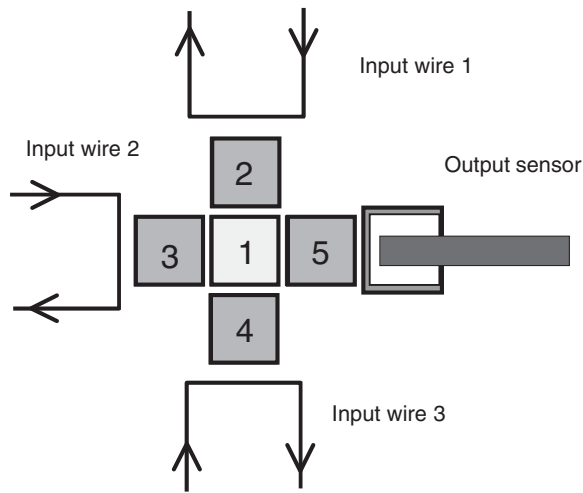


Figure 9. Physical layout of the majority gate.

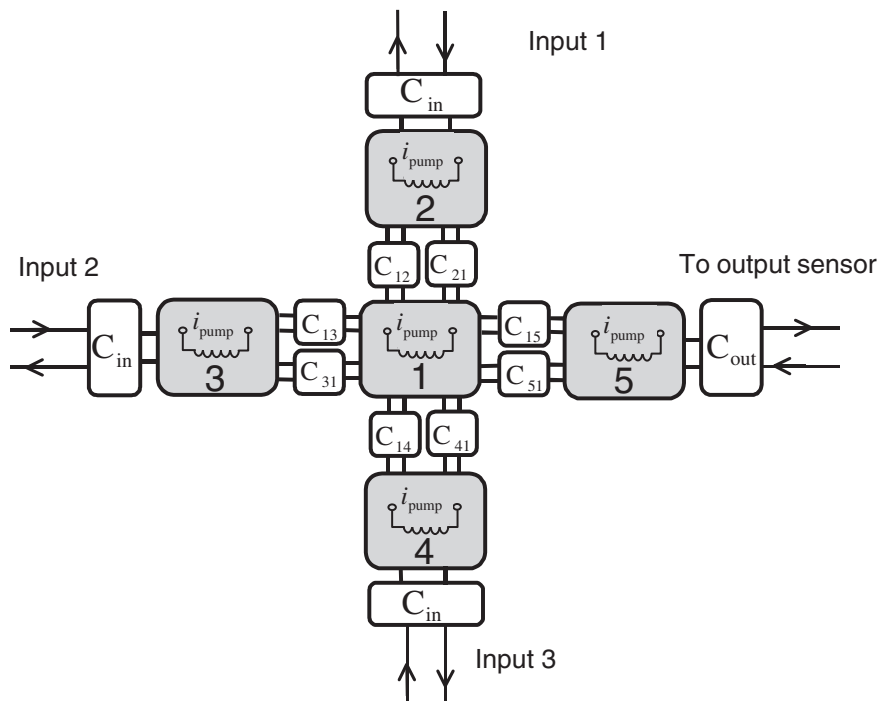


Figure 10. Circuit schematics of the majority gate. Each dot is inductively coupled to its nearest neighbour and to the external field.

Logic gates are realized by dots driven by multiple inputs. The layout of the so-called magnetic majority gate is shown in Figures 9 and 10. A similar pumping scheme is used to drive this structure to ground state. If one of the input dots is in logical '1' state, the dot realizes a logical NOR function between the other two inputs and the output, and if one input is in logical '0', then the gate computes the NAND function. In this example, the state of the inputs is determined directly by currents, in a complex array the inputs come from output dots of other majority gates and magnetic wires.

The demagnetization factors of the output dot can be designed to be different from other dots in the structure, resulting in a lower switching field. It assures that this dot is the first dot to make the transition to the neutral logic state and the last to switch back to a definite logic value in the adiabatic control scheme. The fact that a homogenous external field can 'target' similarly shaped specific dots inside a larger array is the key for the design of complex, sequential logic circuits.

5. CONCLUSIONS AND OUTLOOK

We demonstrated, how circuit concepts could be applied to design simple signal-processing devices from coupled ferromagnetic dots. Operating logic devices were shown as examples of such design. These digital 'circuits' are only one possible application of the nanomagnet devices; the transistor-like hysteresis behaviour might be applied in analog processors as well.

We developed our circuit models based on the single domain approximation (Stoner–Wohlfarth model). Small-size (but not single domain) particles also show the transistor-like behaviour of Figure 3, and the basic concepts of this paper remain valid even if the single domain approximation breaks down. Different realizations than single domain nanodots also help to eliminate a serious difficulty in the realization of nanomagnet circuits namely, that the input-output characteristics (Figure 3) are rather sensitive to the shape of nanomagnet.

Thermal stability is the main factor limiting the miniaturization of the nanomagnet devices. The coupling energy between dots and the energy barrier between the steady states of an individual dot has to be larger than several kT (k is the Boltzmann constant and T is the actual operating temperature). This gives a lower bound for the size of the dots. Permalloy nanomagnets smaller than 40 nm are not stable at room temperature. This size limit yields to an impressive integration density of 10^{10} dots/cm². Each time the dot adiabatically switches, it dissipates at least the few kT energy separating its two steady-states, i.e. the dissipation per bit operation is a few kT . The switching speed can be estimated from the dynamical equation (5) and turns out to be on the sub-nanosecond timescale for typical field. The devices introduced in this publication are adiabatically controlled and the fast, transient dynamics are suppressed—it reduces their speed to few hundred MHz.

Technologies for realizing arrays of nanomagnets (like the one shown in Figure 2) are currently under development for ultra-high density hard disk drives. The construction of input–output circuits is very similar to the read–write structures of novel magnetic memory (MRAM) devices [11]. We believe, that the devices we envisioned can be built on this existing technological basis.

The dissipation and minimum device size is linked to the actual operating temperature, both quantity scales inverse-proportionally with the absolute temperature. This makes this computing architecture especially well suited for low-temperature applications.

ACKNOWLEDGEMENTS

Authors are grateful to G.H. Bernstein and A. Imre for the development of tools for fabrication and characterization of nanomagnets. This work was supported in part by Office of Naval Research (MURI program) and the W. M. Keck Foundation.

APPENDIX A: STATIC MICROMAGNETICS OF SINGLE DOMAIN PARTICLES

In this section, we give a concise summary of static micromagnetics, with special emphasis on the equilibrium state of a single domain nanomagnet in static external magnetic field [5,6].

Static micromagnetics describes the magnetic field, in the presence of ferromagnetic materials, produced by time-independent field sources. According to Maxwell's equations, external current sources \mathbf{J}_s generate rotation of the magnetic field \mathbf{H} , the divergence of the magnetic flux density \mathbf{B} is zero, and the magnetization vector \mathbf{M} of the material defines the relation between \mathbf{B} and \mathbf{H} :

$$\text{rot } \mathbf{H} = \mathbf{J}_s; \quad \text{div } \mathbf{B} = 0; \quad \mathbf{B} = \mu_0(\mathbf{H} + \mathbf{M}) \quad (\text{A1})$$

In Equation (A1) \mathbf{H} is the sum of the externally applied magnetic field \mathbf{H}_{ext} and the dipole magnetic field generated by the magnetized material, referred to as \mathbf{H}_d .

Inside a bulk material, the interplay of four different magnetic forces, namely the force between magnetic dipoles, the quantum exchange force, the anisotropy force, and the externally applied forces determine the equilibrium. This interplay results in a domain structure, i.e. distinct regions of spontaneously magnetized in distinct directions. The magnitude of the magnetic moment $M_S = |\mathbf{M}|$ at a given temperature is constant everywhere in the sample. Magnetization equilibrium in a material corresponds to a minimum of free energy density of the medium, or equivalently, the vanishing of the magnetic torque per unit volume acting in the medium.

The domain structure, including the number of domains, depends on the size of the sample. In sufficiently small particles, the strong exchange force does not allow more than one domain to develop, the sample behaves as a 'single domain' particle. In the following, we shall assume that we are dealing with single domain nanomagnets, in which the magnetization direction is uniform, or at least it is approximately uniform.

A single domain nanomagnet cannot be demagnetized. It is always magnetized to the saturation magnetization, M_S . However, the direction of \mathbf{M} changes in response to an applied field, and it tends to turn the magnetization towards the field direction.

The total energy of a magnetic specimen is obtained by summing the quantum exchange energy, the magnetocrystalline anisotropy energy and the magnetostatic energy. The spatial dependence of the exchange energy is local. Its strength at a given point depends only on the magnetization around this point. However, the interaction between magnetic dipoles is a long-range interaction. Its value at a given point depends on the magnetization over the whole volume of the magnetic material.

In micromagnetics, to represent the effects of the different energy terms on the magnetization vector, an 'effective magnetic field' is introduced

$$\mathbf{H}_{\text{eff}} = \mathbf{H}_{\text{exch}} + \mathbf{H}_d + \mathbf{H}_{\text{ext}} \quad (\text{A2})$$

where

$$\mathbf{H}_{\text{exch}} = \frac{2A_{\text{exch}}}{M_S^2} \nabla^2 \mathbf{M} \quad (\text{A3})$$

where A_{exch} is called ‘exchange stiffness’; \mathbf{H}_d stands for the self-demagnetization of the sample and

$$\mathbf{H}_d = -\text{grad } \Phi_d, \quad \text{where } \Phi_d = \frac{1}{4\pi} \left[-\int \frac{\text{div } \mathbf{M}}{|\mathbf{r} - \mathbf{r}'|} dV' + \int \frac{\mathbf{M}\mathbf{n}}{|\mathbf{r} - \mathbf{r}'|} dS' \right] \quad (\text{A4})$$

originating from the dipole–dipole interactions. \mathbf{H}_{ext} is the externally applied magnetic field. We do not deal with possible additional terms (for considering magnetic anisotropy, thermal fluctuations, etc.) that can be added to Equation (A2) to generalize the model.

The total energy of the material sample can be given as

$$E_{\text{total}} = \frac{1}{2} \mu_0 \int_V \mathbf{H}_{\text{eff}} \mathbf{M} dV \quad (\text{A5})$$

At equilibrium, the first variation δE_{total} must vanish, the second variation $\delta^2 E_{\text{total}}$ must be positive.

For deep-submicron size magnetic particles the exchange interaction makes the magnetization distribution uniform inside the particle. The exchange term vanishes from expression (A2) and (A3) reduces to a surface integral. Moreover, since $\mathbf{M}^{(i)}$ is a constant for a particular dot, it can be moved outside any integration or differentiation with respect to spatial co-ordinates [5]. Therefore, the magnetostatic energy of a dot (which dot is denoted by superscript (i)) can be expressed as:

$$\begin{aligned} E_{\text{total}}^{(i)} &= E_{\text{demag}}^{(i)} + E_{\text{coupling}}^{(i)} + E_{\text{zeeman}}^{(i)} \\ E_{\text{zeeman}}^{(i)} &= \frac{1}{2} \mu_0 V^{(i)} \mathbf{M}^{(i)} \mathbf{H}_{\text{ext}} \\ E_{\text{demag}}^{(i)} &= \frac{1}{2} \mu_0 V^{(i)} \mathbf{M}^{(i)} \mathbf{H}_{\text{demag}}^{(i)} = \frac{1}{2} V^{(i)} (-\mathbf{N}^{(i)} \mathbf{M}^{(i)}) \mathbf{M}^{(i)} \\ E_{\text{coupling}} &= \frac{1}{2} \mu_0 V^{(i)} \mathbf{M}^{(i)} \mathbf{H}_{\text{coupling}}^{(i)} = \frac{1}{2} V^{(i)} \mathbf{M}^{(i)} \sum_{j \in \text{neighbours}, j \neq i} \mathbf{C}^{(ij)} \mathbf{M}^{(j)} \end{aligned} \quad (\text{A6})$$

Here $V^{(i)}$ is the volume of the nanomagnet, E_{zeeman} represents the energy contribution of the external field E_{demag} is the demagnetization energy, and E_{coupling} is the energy term coming from the interaction with neighbouring dots. The magnetometric demagnetization tensor \mathbf{N} depends on the shape of the dot, and the coupling tensor \mathbf{C} is on the distance and shape of the interacting particles. Note, that as far as the energy is concerned, the single domain dots behave exactly like if they were experiencing a homogenous coupling and demagnetizing field. In other words, the energy defines an averaging over the otherwise non-uniform magnetic fields.

In order to relate parameters \mathbf{N} and \mathbf{C} to the geometry of the structure, we give them for a special case. For a prolate rotational ellipsoid with axes c, c, a the demagnetization tensor

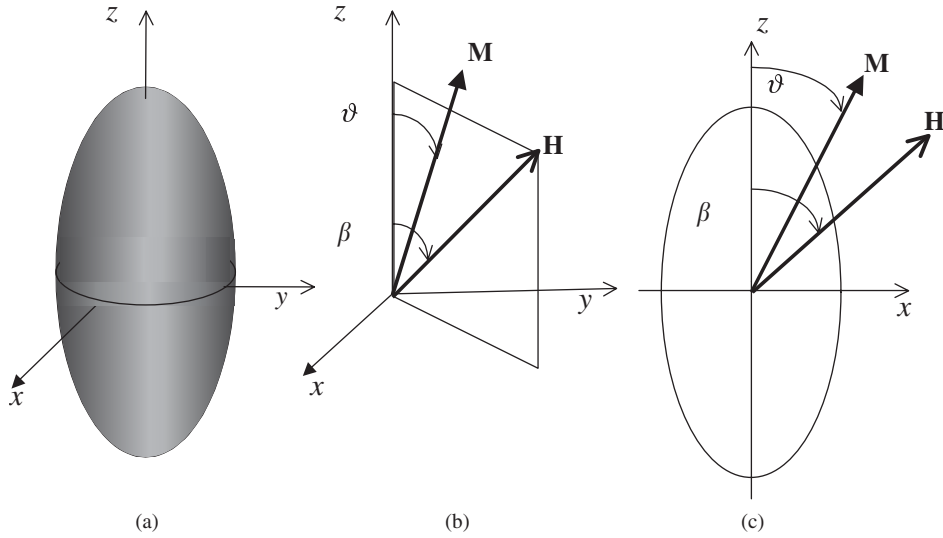


Figure A1. Ellipsoidal nanomagnet in the transformed co-ordinate system.

is diagonal and its elements are given by [6]:

$$\mathbf{N} = \begin{bmatrix} N_x & 0 & 0 \\ 0 & N_y & 0 \\ 0 & 0 & N_z \end{bmatrix}$$

$$\alpha = \frac{c}{a} < 1$$

$$N_z = \frac{\alpha^2}{\alpha^2 - 1} \left[1 - \frac{1}{\sqrt{\alpha^2 - 1}} \arcsin \left(\frac{\sqrt{\alpha^2 - 1}}{\alpha} \right) \right]$$

$$N_x = N_y = \frac{1}{2}(1 - N_z) \quad (\text{A7})$$

The numbers N_x, N_y, N_z are called demagnetizing factors, are positive and obey the condition $N_x + N_y + N_z = 1$. In order to keep our formulas simpler, we always assumed a diagonal demagnetization tensor in developing the circuit model.

The point-dipole approximation gives a simple expression for the coupling matrix between the two dots (i) and (j) [6]:

$$\mathbf{C}^{(ij)} = \frac{V^{(j)}}{4\pi r_{ij}^3} \begin{bmatrix} 3\hat{r}_x^2 - 1 & 3\hat{r}_x\hat{r}_y & 3\hat{r}_x\hat{r}_z \\ 3\hat{r}_y\hat{r}_x & 3\hat{r}_y^2 - 1 & 3\hat{r}_y\hat{r}_z \\ 3\hat{r}_z\hat{r}_x & 3\hat{r}_z\hat{r}_y & 3\hat{r}_z^2 - 1 \end{bmatrix} \quad (\text{A8})$$

where \hat{r} is the unit vector pointing from dot (i) to dot (j) and r_{ij} is their distance.

As an illustration, we will examine the static magnetization behaviour of a single domain ellipsoidal particle shown in Figure A1. The particle will have smaller demagnetizing factors along longer axes. Thus demagnetization creates shape anisotropy in the nanomagnet. In case no crystalline anisotropy is present, the axis that corresponds to smaller demagnetization factors is called ‘easy magnetization’ axis of the nanoparticle.

According to the Stoner–Wohlfarth model, in static equilibrium the \mathbf{M} magnetization vector lies in the $\mathbf{H}_{\text{ext}}-z$ plane. If we turn the co-ordinate system in such a way, that \mathbf{H}_{ext} and \mathbf{M} lie in the $y-z$ plane, then

$$\mathbf{H}_{\text{ext}} = H_0 \sin \beta \mathbf{j} + H_0 \cos \beta \mathbf{k} \quad (\text{A9})$$

and

$$\mathbf{M} = M_S \sin \vartheta \mathbf{j} + M_S \cos \vartheta \mathbf{k} \quad (\text{A10})$$

The energy of the nanomagnet depends on the angle ϑ . Thus in equilibrium the first derivative of the energy with respect to ϑ should be zero and the second derivative should be positive:

$$\frac{1}{2} \sin[2(\vartheta - \beta)] + h \sin \vartheta = 0 \quad \text{and} \quad \cos[2(\vartheta - \beta)] + h \cos \vartheta > 0 \quad (\text{A11})$$

where $h = H_0/M_S(N_x - N_z)$

Hysteresis curves, like the one shown in Figure 3, can be calculated from Equation (A11). Since the equations might have multiple solutions, determination of the magnetic state always requires information about the magnetization history of the sample.

Note, that the points of the hysteresis are also characterized by zero torque henceforth the steady-state solutions can also be calculated from the

$$\mathbf{M} \times \mathbf{H} = 0 \quad (\text{A12})$$

condition.

APPENDIX B: MICROMAGNETIC DYNAMICS

Micromagnetic dynamics is intended to answer the question, how a classical magnetization distribution $\mathbf{M}(\mathbf{r}, t)$ changes in time under the influence of an external magnetic field $\mathbf{H}_{\text{ext}}(\mathbf{r}, t)$. The dynamics of $\mathbf{M}(\mathbf{r}, t)$ is described by the Landau–Lifshitz equation:

$$\frac{\partial \mathbf{M}(\mathbf{r}, t)}{\partial t} = -\gamma \mathbf{M}(\mathbf{r}, t) \times \mathbf{H}_{\text{eff}}(\mathbf{r}, t) - \frac{\alpha \gamma}{M_S} [\mathbf{M}(\mathbf{r}, t) \times (\mathbf{M}(\mathbf{r}, t) \times \mathbf{H}_{\text{eff}}(\mathbf{r}, t))] \quad (\text{B1})$$

Here γ is the gyromagnetic ratio ($\gamma = 2.210 \times 10^5 \text{ T}^{-1} \text{ s}^{-1}$) and α is a damping constant.

Steady-state solutions are local energy minima of the system and physically means stable domain configurations.

This system of partial differential equations almost always calls for numerical evaluation [12]. Several software packages are available [13].

In the single domain approximation, the magnetization distribution ($\mathbf{M}(\mathbf{r}, t)$) replaces with a single magnetization vector for each dot ($\mathbf{M}^{(i)}(t)$), and the single domain Landau–Lifshitz

equation results as

$$\frac{d\mathbf{M}^{(i)}(t)}{dt} = -\gamma\mathbf{M}^{(i)}(t) \times \mathbf{H}_{\text{eff}}^{(i)}(t) - \frac{\alpha\gamma}{M_S} [\mathbf{M}^{(i)}(t) \times (\mathbf{M}^{(i)}(t) \times \mathbf{H}_{\text{eff}}^{(i)}(t))] \quad (\text{B2})$$

The effective field is defined by Equation (A6)

$$\mathbf{H}_{\text{eff}}^{(i)} = \mathbf{H}_{\text{ext}}^{(i)} - \mathbf{N}^{(i)}\mathbf{M}^{(i)} + \sum_{j \in \text{neighbours}, j \neq i} \mathbf{C}^{(ij)}\mathbf{M}^{(j)} \quad (\text{B3})$$

REFERENCES

1. Coey JMD. Magnetism in future. *Journal of Magnetism and Magnetic Materials* 2000; **226–230**:2197–2112.
2. Koo H, Dryer M, Metlushko VV, Gomez RD. Investigation of the Magnetic Interaction of Small Permalloy Particles. *IEEE Transactions on Magnetics* 2001; **37**:2049–2051.
3. Sarid, D. *Scanning Force Microscopy: With Applications to Electric, Magnetic, and Atomic Forces*. Oxford University Press: New York, 1994.
4. Brown WF Jr. *Magnetostatic Principles in Ferromagnetism*. North-Holland: Amsterdam, 1962.
5. Aharoni A. *Introduction to the Theory of Ferromagnetism*. Oxford University Press: Oxford, 2000.
6. Hubert A, Schafer R. *Magnetic Domains*. Springer-Verlag: Berlin, Heidelberg, 1998.
7. Oti JO. *Micromagnetics*. In Webster J (ed.). *Wiley Encyclopedia of Electrical and Electronic Engineering Online*. Wiley: New York, 2000.
8. Allwood DA, Gang Xiong, Cooke MD, Faulkner CC, Atkinson D, Vernier N, Cowburn RP. Submicrometer ferromagnetic NOT gate and shift register. *Science* 2002; **296**:2003–2006.
9. Csaba G, Porod W. Simulation of field coupled architectures based on magnetic dot arrays. *Journal of Computational Electronics* 2002; **1**:1–5.
10. Csaba G, Imre A, Bernstein GH, Porod W, Metlushko VV. Signal processing with coupled ferromagnetic dots. *Proceedings IEEE-NANO*, 2002.
11. Prinz GA. Magnetolectronics. *Science* 1998; **282**:1660–1663.
12. Fidler J, Schrefl T. Micromagnetic modeling—current state of the art. *Physica D* 2000; **33**:R135–R156.
13. Donahue MJ, Porter DG. OOMMF User's Guide, Version 1.0. *Interagency Report NISTIR 6376*, online: <http://math.nist.gov/oommf/>
14. Lent CS, Tougaw PD, Porod W, Bernstein, GH. Quantum cellular automata. *Nanotechnology* 1993; **4**:49–57.